

# Optimizing Aerofoil Design: A Comprehensive Analysis of Aerodynamic Efficiency through CFD Simulations and Wind Tunnel Experiments

Anant Sidhappa Kurhade<sup>1\*</sup>, Gulab Dattrao Siraskar<sup>2</sup>, Ganesh E. Kondhalkar<sup>3</sup>,  
Milind Manikrao Darade<sup>4</sup>, Rahul Shivaji Yadav<sup>5</sup>, Ramdas Biradar<sup>6</sup>, Shital Yashwant Waware<sup>1</sup> and  
Girish Anant Charwad<sup>7</sup>

<sup>1</sup>Department of Mechanical Engineering, Dr. D. Y. Patil Institute of Technology, Pimpri, Pune - 411018, Maharashtra, India; [a.kurhade@gmail.com](mailto:a.kurhade@gmail.com)

<sup>2</sup>Department of Mechanical Engineering, PCET's Pimpri Chinchwad College of Engineering and Research, Ravet, Pune - 412101, Maharashtra, India

<sup>3</sup>Department of Mechanical Engineering, ABMSP's Anantrao Pawar College of Engineering and Research, Parvati, Pune - 411009, Maharashtra, India

<sup>4</sup>Civil Engineering Department, Nagnathappa Halge College of Engineering, Parli Vaijnath - 431515, Maharashtra, India

<sup>5</sup>Department of Mechanical Engineering, Marathwada Mitramandal's College of Engineering, Karvenagar, Pune - 411052, Maharashtra, India

<sup>6</sup>School of Engineering & Technology, PCET's Pimpri Chinchwad University, Sate, Pune - 412106, Maharashtra, India

<sup>7</sup>Department of Applied Art, Bharati Vidyapeeth's College of Fine Arts, Pune - 411043, Maharashtra, India

## Abstract

*This study explores the aerodynamic properties of different aerofoil shapes and their performance under varying flow conditions to identify the most efficient design based on lift-to-drag ratio, stall behaviour, and overall aerodynamic efficiency. Using Computational Fluid Dynamics (CFD) simulations, several aerofoil profiles were analysed at different angles of attack and flow speeds. These simulations were validated through wind tunnel experiments, offering a comprehensive understanding of aerofoil performance in real-world scenarios. The combination of CFD analysis and wind tunnel testing enabled a thorough assessment of each aerofoil shape, leading to the discovery of a specific aerofoil with a high lift-to-drag ratio and stable performance at high angles of attack. These results have significant implications for the design of wings and blades in aerospace and aeronautical applications, improving fuel efficiency and performance in both aviation and wind energy sectors. Additionally, dynamic roughness shows potential in reducing separation bubbles, but further investigation is needed to assess its effectiveness at higher angles of attack and elevated Reynolds numbers. Understanding the scalability and practical application of dynamic roughness in real-world scenarios is essential. Current research on surface modifications like dimples and riblets lacks optimized configurations for varying conditions. More research is needed to understand the interaction between surface geometries and the boundary layer, particularly at higher angles of attack and Reynolds numbers. Combining experimental and numerical methods can provide a comprehensive understanding of flow control techniques. The limited*

\*Author for correspondence

research on applying flow control strategies to wind turbine blades indicates a significant opportunity to improve wind energy efficiency. Future studies should focus on optimizing multiple techniques and addressing practical challenges, such as durability, cost-effectiveness, and integration into existing systems. Investigating the cost-effectiveness and durability of these modifications for long-term use will be vital for their successful adoption in the industry. Expanding research to include the effects of environmental factors like temperature and humidity will offer a more complete understanding of flow control in various operating conditions. By addressing these gaps, advancements in aerodynamic performance can be achieved, benefiting the aerospace and wind energy sectors.

**Keywords:** Aerodynamic Properties, Aerofoil Shapes, Flow Conditions, Lift-To-Drag Ratio

## 1.0 Introduction

Energy is crucial for human life, and traditionally, it has been produced primarily from fossil fuels. However, these sources have limitations due to their finite availability and their contribution to environmental pollution. In India, burning 1 to 2 million tons of coal daily for power generation is a major source of greenhouse gas emissions. As population and electricity consumption grow, renewable energy must increasingly fill the gap. Consequently, renewable energy presents a viable alternative, with wind power emerging as one of the leading sources. Wind energy stands out as a sustainable, competitive option, gaining more recognition as an effective replacement for conventional energy sources. Capturing wind energy is essential, as wind turbines convert it into mechanical and then electrical energy. The wind turbine blade shape is a key factor in harnessing wind power effectively. However, the efficiency of wind turbines can be improved. To enhance performance, scientists are researching various aspects of wind turbines and their components. Proper planning and research are

needed when establishing wind turbines to maximize power output under specific atmospheric conditions. The aerofoil profile is a crucial element in wing design, as the wing's efficiency depends heavily on this profile. Aerodynamics at low Reynolds numbers plays a vital role in various applications such as wind turbines, UAVs, sailplanes, and jet engine fans. The increasing popularity of UAVs and Micro Air Vehicles (MAVs) calls for in-depth research into the aerodynamics of both 2D aerofoils and 3D wings. To address this, examining various aerofoil profiles is crucial for enhancing performance. One strategy is to focus on small, simple wind turbines for power generation in low-wind areas. While less efficient than larger systems, these turbines require minimal industrial infrastructure and can generate power on-site, simplifying the electrical grid. Therefore, it's important to analyse aerofoil behaviour at low Reynolds numbers.

### 1.1 Aerofoil Nomenclature

The design of wind turbines primarily depends on the aerodynamic requirements, but it also must be considered

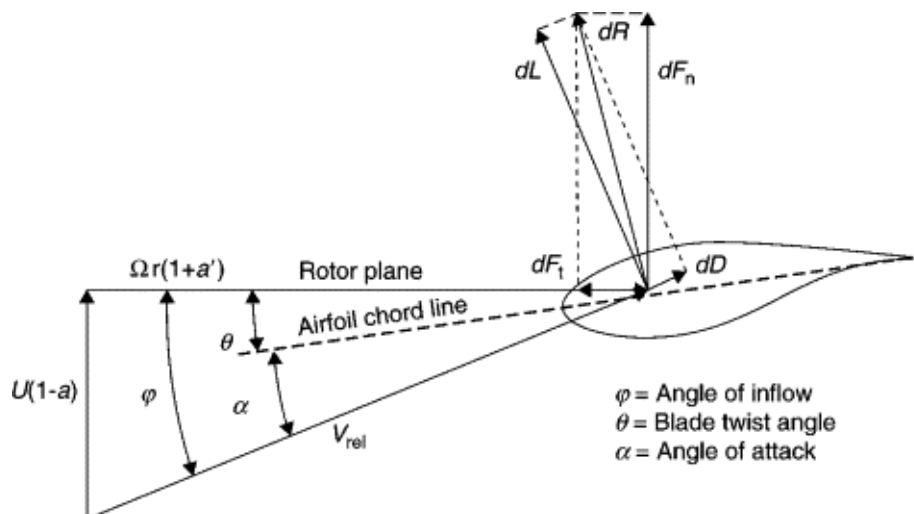
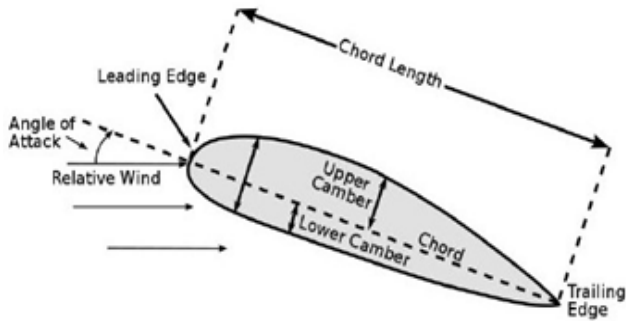


Figure 1. Aerofoil shape of wind turbine blade<sup>1</sup>.



**Figure 2.** Aerofoil nomenclatures.

from an economic point of view. The shape of the wind turbine blade helps to keep the cost of construction reasonable. Figure 1 shows the incorporation of aerofoil shape in wind turbine blades<sup>1</sup>. An aerofoil is the shape of a wing or blade (of a propeller, rotor or turbine) or sail. An aerofoil produces lift (upward force) and drag (resistance) when moving through air. Lift is perpendicular to the motion, while drag opposes it. Aerofoils for subsonic flight are typically curved, with a rounded front and a pointed back.

Figure 2 shows the cross-section of an aerofoil to describe the various terminologies used in aerodynamics. Some important terms related to aerofoil are described below:

## 1.2 Wind Turbine Blade Aerodynamics

Consequently, aerodynamics, the study of how objects interact with air, is essential for wind turbine design. Wind speed is a critical factor affecting turbine performance, as the power generated is directly proportional to the cube of wind velocity. While wind speeds below 5 m/s are generally insufficient for power generation, higher wind speeds can lead to increased turbine loads due to fluctuations. Interestingly, the turbine itself influences wind conditions. As air passes through the turbine, it slows down, reducing the available power. This phenomenon, known as the “disc area effect,” limits the maximum theoretical power capture to approximately 59%, a constraint defined by Betz’s limit. In essence, wind turbine blade design must carefully consider aerodynamic principles to optimize energy extraction while accounting for the complex interactions between the turbine and the wind.

### 1.2.1 Lift and Drag Forces on Aerofoil

Wind turbine blades are designed to generate lift, a force that propels them upwards. This lift is created due to the specific shape of the blade, known as an airfoil. The upper surface of the blade is curved, causing air to flow faster over it compared to the flatter underside. The imbalance in pressure generates an upward force, called lift. This aerodynamic principle is visually depicted in Figure 3<sup>2</sup>.

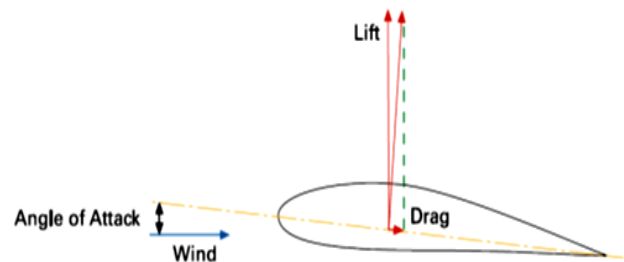


**Figure 3.** Lift and drag forces on aerofoil<sup>2</sup>.

The lift generated by a wind turbine blade increases as the blade’s angle to the wind increases, up to a point. Beyond this optimal angle, the blade stalls, and lift decreases rapidly. This optimal angle is where smooth airflow transitions to turbulent flow. Simultaneously, drag, the force opposing movement, also increases with the angle of attack. Effective blade design maximizes lift while minimizing drag. The ideal operating point is just below the stall angle, where the ratio of lift to drag is highest. Drag, often measured by the drag coefficient, is a force

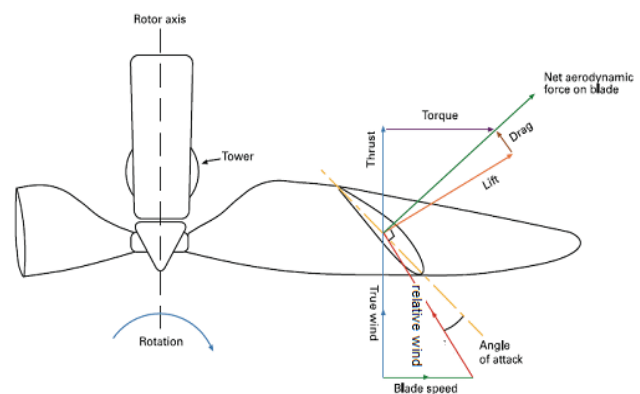


**Figure 4.** Apparent wind angles<sup>2</sup>.

that opposes movement through a fluid. In a stationary turbine, drag might seem inconsequential. However, once the blade rotates, it encounters the apparent wind, a combination of the true wind and the blade's motion. This alters the angle of attack, reducing lift and increasing drag, impacting overall turbine efficiency shown in Figure 4<sup>2</sup>.

### 1.2.2 Twist

The twisting of wind turbine blades adjusts the angles of attack, like how an aerofoil behaves at various angles of attack in aerodynamics. As the blade moves closer to the tip, its speed through the air increases, resulting in a greater apparent wind angle. Therefore, the blade must be twisted more at the tips than at the root, ensuring an optimal angle of attack along its entire length.

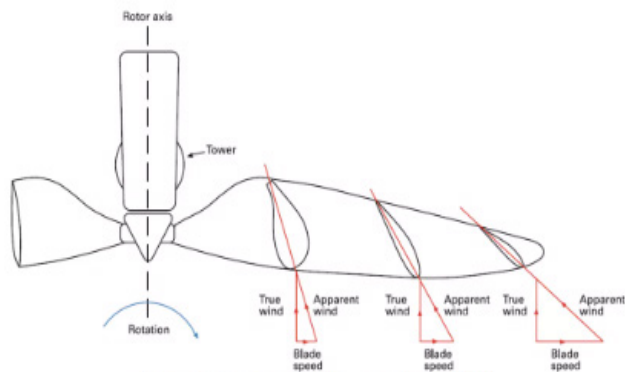


**Figure 5.** Twisting of blades<sup>3</sup>.

Figure 5. This twist is necessary because the blade's tip travels faster than the segments closer to the rotor hub. Straight blades, which do not have this twist, are simpler and cheaper to manufacture. Typically, wind turbine blades have a twist ranging from around 10° to 20° from root to tip.

### 1.2.3 The Process of Flow Separation

At low speeds (low Reynolds numbers), the air flowing over an aerofoil tends to remain smooth (laminar) until the air pressure starts to increase. This smooth airflow significantly affects the aerofoil's performance. However, smooth airflow cannot handle sudden increases in air pressure. This separation reduces the aerofoil's efficiency, increasing drag and decreasing lift.

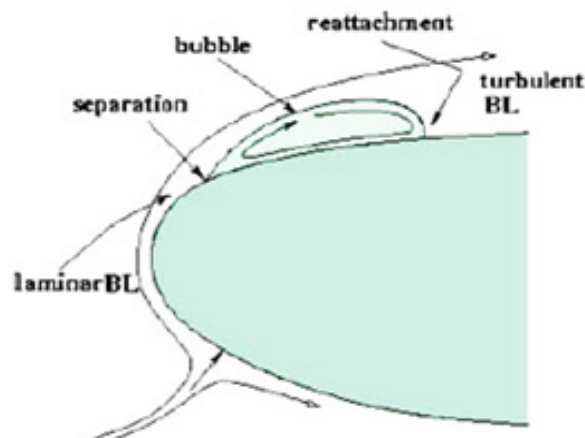


**Figure 6.** Laminar separation formed<sup>4</sup>.

In some cases, the separated airflow can become turbulent due to the strong pressure increase. Interestingly, this turbulence can sometimes cause the airflow to reattach to the aerofoil, forming a bubble of separated airflow. This phenomenon is illustrated in Figure 6.

Once the turbulent flow re-attaches to the aerofoil, it continues to adhere to the surface until the aerofoil's trailing edge. However, as the aerofoil's angle increases, the airflow can separate again, forming a bubble of slow-moving air. This separation can lead to a stall, where the aerofoil suddenly loses lift.

The size and shape of this separation bubble depend on various factors, including the aerofoil's shape, angle of attack, and air conditions. As the angle of attack increases, the bubble becomes smaller and moves closer to the aerofoil's leading edge. Eventually, the bubble bursts and the airflow separates. Despite this, the separated flow often reattaches further downstream on the aerofoil.

This study aims to identify the most efficient aerofoil design by analyzing aerodynamic properties under varying flow conditions using CFD simulations and wind tunnel experiments, while also exploring the potential of dynamic roughness and surface modifications to enhance aerodynamic performance and energy efficiency in aerospace and wind energy applications.

## 2.0 Literature Review

Hui Hu *et al.*<sup>4</sup> studied how air flowed over a specific aerofoil at low speeds. They used detailed measurements

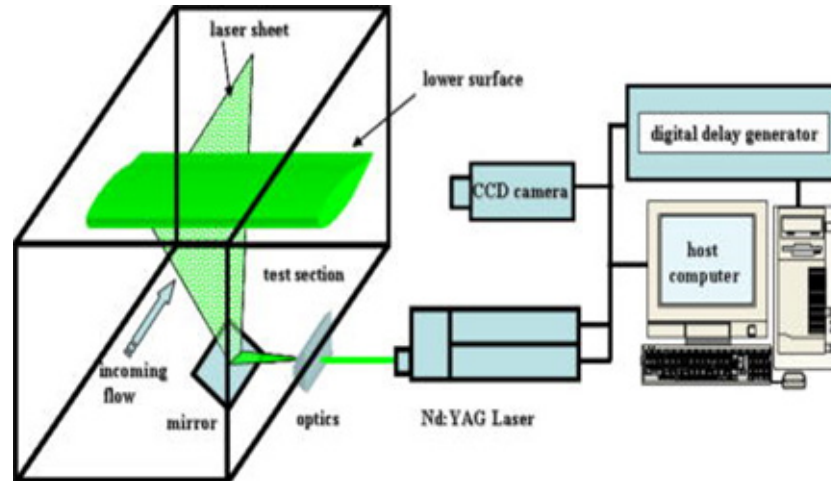


Figure 7. Setup for the PIV measurements<sup>4</sup>.

to observe the airflow behavior at different angles. At small angles, the air stayed attached to the airfoil, but as the angle increased, the airflow started to separate. This separation caused a gradual decrease in lift and a rapid increase in drag. When the angle became very large, the separated airflow suddenly burst, leading to a sharp drop in lift and a significant increase in drag, resulting in a stall as shown in Figure 7.

Kurhade *et al.*<sup>5-7</sup> studied smartphones and thermal performance. Anant *et al.*<sup>8-10</sup> used phase change material to minimise the temperature of chips. Shital *et al.*<sup>11-13</sup> provide critical reviews on heat transfer and heat transfer enhancement in tubular heat exchangers with jet impingement. Rahul Khot *et al.*<sup>14-19</sup> explain the investigation of laser welding parameters on the strength of TRIP steel. Gadekar T. D *et al.*<sup>20-22</sup> explain an experimental study on gear EP lubricant mixed with  $\text{Al}_2\text{O}_3/\text{SiO}_2/\text{ZrO}_2$  composite additives to design a predictive system. Patil P *et al.*<sup>23</sup> used a water-based  $\text{Al}_2\text{O}_3$  nanofluid in this work to grind materials due to its outstanding convective heat transfer and thermal conductivity qualities.

Mohammad Mashud *et al.*<sup>24</sup> the study explored a method for controlling aerofoil flow separation by introducing partial bumpy surfaces on its upper side. Historical NACA reports also investigated the impact of surface protuberances on airfoil and wing performance. Optimal aerofoil performance may require altering the boundary layer behaviour or adjusting aerofoil geometry to suit varying free stream conditions. These experiments, conducted with a flow chord-based Reynolds number of approximately 3.1 million, considered variations in the

shape, span, length, height, and position of protuberances. The NACA4315 aerofoil, a relatively thick profile, was tested with a 260 mm chord and 6.35 mm maximum bumpy surface height. Two models were prepared: one with a smooth surface and one with a bumpy surface. Both were made of wood and tested in a  $36 \times 36 \times 100$  cm subsonic wind tunnel. The results showed that flow separation occurred at an  $8^\circ$  angle of attack with the smooth model, while it occurred at  $14^\circ$  with the bumpy model.

This method of controlling airflow has benefits compared to other techniques. Computer simulations were used to study how creating small, moving bumps (dynamic roughness) on the leading edge of an airfoil affects airflow. The simulations involved testing a smooth airfoil to identify areas of separated airflow, followed by testing the airfoil with the added bumps to see how it changed the airflow. These tests were performed at various angles of attack up to 12 degrees. The initial bump was placed near the front of the airfoil, and it was found that small, rapidly moving bumps could effectively control the airflow if they were the right size and speed.

Deepanshu Srivastav<sup>25</sup> two-dimensional CFD simulations were conducted on a wing model with NACA0018 profile, testing both outward and inward dimples at various angles of attack using the k- $\omega$  turbulence model as shown in Figure 8. After selecting the most efficient dimple configuration, different dimple shapes were tested against a plain aerofoil model. The CFD analysis continued in 3D, focusing on a segment of the aerofoil with one dimple. The goal of this research was

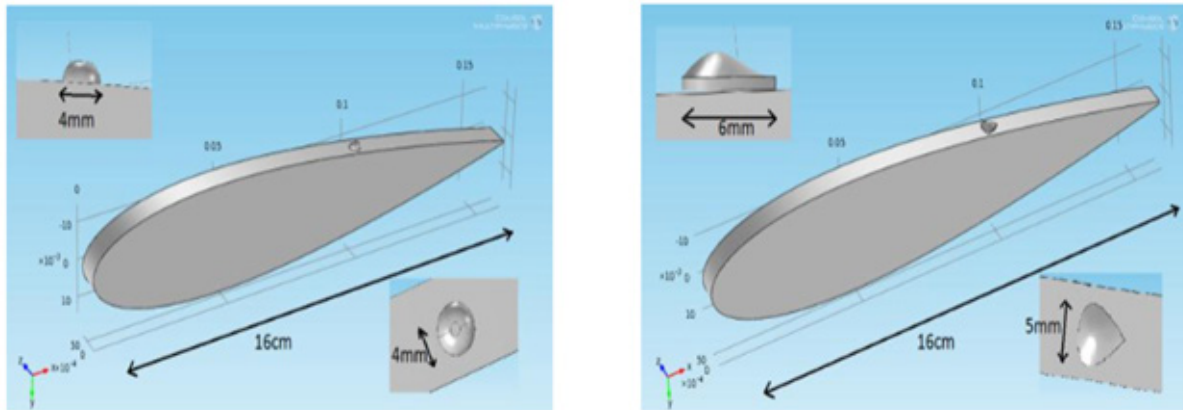


**Figure 8.** NACA 0018 with round and composite dimples<sup>25</sup>.

to enhance aircraft manoeuvrability and performance through airflow control over the airfoil. The  $k-\epsilon$  turbulence model was applied in both 3D and 2D simulations using COMSOL's fluid flow module to assess the flow regime. Triangular meshing was utilized, beginning with coarse settings and progressively refining after each converged solution. All NACA 0018 simulations were conducted at various angles of attack and an inlet velocity of 20 m/s. The 2D simulations compared inward and outward dimples against a smooth NACA0018 aerofoil with an attack angle ranging from -5 to 15 degrees. The outward dimple configuration yielded the lowest drag, prompting its use in 3D simulations.

In 2012, researchers Ji Yao *et al.*<sup>26</sup> conducted a computer simulation to study how well the NACA0018 airfoil, designed for wind turbines, performs in different air conditions. They examined the airflow patterns around the airfoil and compared the results of different mathematical models used to represent air turbulence. The simulations were performed for various angles of attack and specific air density and speed conditions. The study area for the simulation was a half-circle shape with a flat back, where the airfoil was placed near the centre. The computational space was divided into small, structured sections for accurate analysis.

The researchers used four different mathematical models to represent air turbulence in their simulations. These models were used to calculate the airflow characteristics around the airfoil. The results showed that the way air flows over a wind turbine airfoil is crucial for designing and evaluating its performance. Of the four turbulence models used, the one called the Reynolds

stress model produced the most accurate results across different angles of attack. The simulations also revealed that at larger angles of attack, the pressure difference between the top and bottom of the airfoil increased, and the air flowed faster around the airfoil.

In 2013, Shantanu S. Bhat *et al.*<sup>27</sup> experimented to study how a specific airfoil (NACA0012) responds to oscillating movements at low speeds. They measured the forces acting on the airfoil and observed the airflow around it. The airfoil was placed in a water tunnel and moved back and forth at a specific angle. The forces on the airfoil were measured and the airflow was visualized using a technique called particle image velocimetry. The results showed that when the airfoil moved slightly, the patterns of airflow separation were not clear. However, the way the separated airflow moved about the airfoil's movement determined whether the airfoil's oscillations increased or decreased.

In 2013, Lei Juanmian *et al.*<sup>28</sup> studied how air separates from the back edge of a symmetrical airfoil at low speeds using computer simulations. They found that at certain angles, a region of separated air forms and creates two swirling patterns. One swirling pattern is weak and has little effect, while the other is strong and significantly influences the air pressure on the airfoil. The researchers used a specific airfoil shape and a detailed computer model to simulate the airflow. They tested the airfoil at different angles and found that at low angles, air separates from both sides of the airfoil. As the angle increases, a region of separated air forms on the back edge and repeatedly grows, bursts, and sheds.



**Figure 9.** Smooth aerofoil profile and triangular roughness profile<sup>11</sup>.

A. Dhiliban *et al.*<sup>29</sup> the study examined how surface roughness impacts flow over an aerofoil at the trailing edge to reduce drag. When triangular roughness was applied to the lower surface of the aerofoil, the coefficient of lift increased significantly. The highest coefficient of lift was observed when the triangular roughness extended from 60% of the chord length to the trailing edge on the lower surface. The study focused on the NACA 0018 aerofoil profile under subsonic conditions..

Initial experiments were performed on a smooth aerofoil in a wind tunnel before introducing surface roughness. CFD analysis was conducted at angles of attack ranging from -20 to 20 degrees in 5-degree intervals, with a constant velocity of 100 m/s. The standard  $k-\epsilon$  model was used for the numerical simulations. Both experimental and numerical results showed that aerodynamic efficiency improved when triangular roughness was applied from 60% of the chord length to the trailing edge on the lower surface for negative angles of attack, and from 90% of the chord length to the trailing edge for positive angles of attack. P. Ghosh *et al.*<sup>30</sup> conducted a thorough wind tunnel study on an aerofoil, measuring pressure distribution, lift and drag forces, and mean velocity profiles. The findings revealed that lift increased when the aerofoil was closer to the ground compared to higher elevations. Maximum lift was achieved at critical angles of attack between 30 to 90 degrees. The tests were conducted in an open-circuit, suction-type, low-speed wind tunnel at 35 m/s, with fourteen pressure ports on the aerofoil surface measuring pressure using a U-tube manometer. The angle of attack varied from 0 to 12 degrees, and ground

clearances reached up to 8.7 cm. Results indicated zero lift at a zero-degree angle of attack, with lift increasing up to 9 degrees before decreasing for all ground clearances. Karna S. Patel *et al.*<sup>31</sup> performed CFD analysis on the NACA 0012 aerofoil at 0- and 6-degree angles of attack using the transition SST model with a free stream velocity of 50m/s. The flow domains were divided into smaller subdomains, and contour plots of static pressure and velocity were created. The static pressure contour at 0 degrees showed the stagnation point at the aerofoil's nose, while at 6 degrees, it was just below the leading edge, creating lift due to a low-pressure region on the upper surface. The lift coefficient increased with the angle of attack up to a peak and then decreased, with airflow separation becoming more noticeable at higher angles. The CFD analysis concluded that no lift was produced at 0 degrees but increasing the angle of attack improved lift force. Agrim Sareen *et al.*<sup>32</sup> evaluated the DU 96-W-180 aerofoil with four symmetrical V-shaped riblet sizes (44, 62, 100, and 150  $\mu\text{m}$ ) across three Reynolds numbers ( $1 \times 10^6$ ,  $1.5 \times 10^6$ , and  $1.85 \times 10^6$ ) and various angles of attack in the aerofoil's low drag range. Testing was done in the UIUC low-turbulence subsonic wind tunnel, with a rectangular test section measuring 2.8 x 4.0 ft (0.853 x 1.219 m) and a length of 8 ft (2.438m). The test-section speed could be adjusted up to 160 mph (71.53m/s) using a 125-hp AC motor and a five-bladed fan. Pressure coefficient graphs showed natural transition occurring around 40% chord on the upper surface and 75% chord on the lower surface. Surface oil flow visualization identified a laminar separation bubble starting at 38% chord and

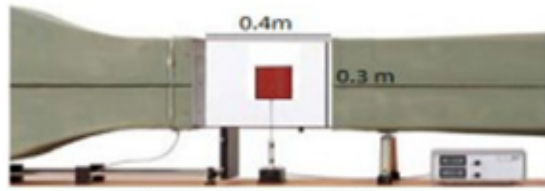
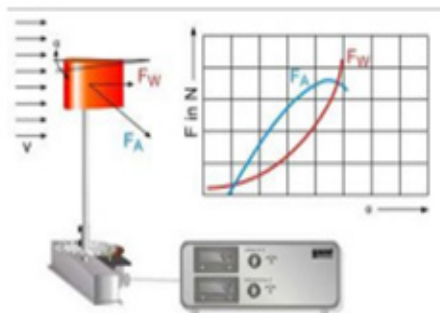


Fig. 1-a. Wind tunnel test area.



Fig. 1-b. Airfoil details.

Figure 10. Wind tunnel test mechanism<sup>34</sup>.

reattaching at 45% chord. The study found that drag reduction depended on factors such as angle of attack, Reynolds number, riblet size, and riblet placement, with a  $62 \mu\text{m}$  riblet size providing optimal performance. Syed Hasib Akhter Faruqui *et al.*<sup>33</sup> explored controlling flow separation on an aerofoil by adding partial dimples to its upper surface. Two models were analyzed: one with a smooth surface and one with dimples on the upper surface near the trailing edge (around 80% of the chord length). Numerical analysis used two-equation turbulence models and a C-type mesh. Flow separation was not observed at zero degrees for either model. However, as the angle of attack increased from 0 to 12 degrees, flow separation began at approximately 70% to 75% of the chord length. The dimpled surface delayed flow separation, occurring at a 15-degree angle of attack compared to 9 degrees for the smooth surface. Izzet Şahin and Adem Acir<sup>34</sup> conducted both numerical and experimental analyses of lift and drag performance for the NACA0015 aerofoil at various angles of attack under low Reynolds numbers, as shown in

Figure 10. Forces were measured every two degrees from  $0^\circ$  to  $20^\circ$ . Experiments were performed in a low-speed wind tunnel, with wind velocity ranging from 3 m/s to 28 m/s. Stationary plates with a 1 mm gap maintained two-dimensional flow, and tests were conducted at 10 m/s. The aerofoil was connected to an electronic two-component coefficient transducer, with drag and lift values displayed digitally.

The angle of attack was adjusted using a graduated dial. For CFD analysis, Spalart-Allmaras and K-epsilon models were employed, and the results were compared with experimental data. In the FLUENT program, the top, bottom, and left boundaries were positioned 10 chords away from the aerofoil, while the right boundary was placed 20 chords away. A mesh independence study was performed to ensure the solution would not change with further refinements, resulting in the use of 33,600 grids for the aerofoil model. The findings revealed that both drag and lift coefficients increased with a rising angle of attack. The stall occurred at an angle of attack of  $16^\circ$ . When the aerofoil reached stall, the lift coefficient decreased, while the drag coefficient increased. Bhushan Patil and Hitesh Thakare<sup>35</sup> the NACA0012 profile was used to analyze the wind turbine blade, with lift and drag forces calculated at various angles of attack for Reynolds numbers ranging from 10,000 to 800,000 through CFD analysis. A C-type mesh with a two-way velocity inlet method was employed in the current analysis. The pressure-based implicit steady solver, along with a standard k- $\epsilon$  model using the PRESTO second-order upwind scheme, was used for the analysis. The results were validated against experimental data from a Sandia National Laboratory Energy report. It was found that while the CFD results for the coefficient of lift showed some deviation from the experimental data at lower angles of attack, they closely matched the experimental results at higher angles of attack. The study concluded that as the Reynolds number increased, lift and drag forces also increased. Both CFD and experimental results demonstrated that the NACA0012 profile provides maximum lift and drag at higher Reynolds numbers. Anshuman Yadav *et al.*<sup>36</sup> the study outlined the theory behind the construction and design of horizontal axis wind turbine blades, focusing on the potential for implementing small wind turbines in residential areas. The researchers compared the performance characteristics of NACA4412 and NACA0012 wind turbine aerofoils.



Sagwan wood was chosen as the material for the wind turbine blades. The output power was measured using multimeter readings. The results indicated that the output power of horizontal axis wind turbines with NACA4412 and NACA0012 blades is directly proportional to the cube of the wind velocity impacting the blade. Additionally, the findings revealed that the average output power of the NACA4412 aerofoil was higher than that of the NACA0012 aerofoil. Ankan Dash<sup>37</sup> the study analyzed the NACA0012 wind turbine aerofoil by maintaining a constant Reynolds number while varying angles of attack. An unstructured mesh with a sphere of influence centred on the middle of the aerofoil was chosen for discretizing the computational domain. A pressure-based steady-state solver with the realizable k-epsilon turbulence model was utilized for the analysis. The flow velocity was set at 50 m/s, with angles of attack at 4, 6, 8, and 10 degrees. The CFD simulations produced contours of velocity and pressure distribution. The results showed an increase in both lift and drag coefficients, though the rise in drag was less pronounced compared to the increase in lift force. Additionally, the greater pressure on the lower surface of the aerofoil, compared to the incoming flow stream, effectively pushed the aerofoil upward, perpendicular to the incoming flow stream.

### 3.0 Area of Opportunity

Research on dynamic roughness has shown promise in eliminating separation bubbles at moderate angles of attack, but its effectiveness at higher angles and Reynolds numbers requires further investigation. Understanding the scalability and practical application of dynamic roughness in real-world scenarios is also essential. Various studies have explored surface modifications like dimples, riblets, and roughness elements to control flow separation. However, there's a gap in determining the optimal configuration of these modifications across different airfoil profiles, Reynolds numbers, and angles of attack. The impact of surface geometry, including partial bumpy surfaces and dimples, on delaying flow separation has been examined. However, further investigation is needed to understand how different surface geometries interact with the boundary layer, especially at higher angles of attack and Reynolds numbers.

Tahzib *et al.*<sup>38</sup> suggested that suggest that higher TSR generally enhances aerodynamic performance across most scenarios, particularly at lower blade pitch angles. However, the study concludes that a VAWT with S1046 aerofoils set at a -2-degree blade pitch and operating at a TSR of 4 achieves optimal performance. Khaoula Qaissi *et al.*<sup>39</sup> indicate that flow remains attached in the pre-stall region, with separation starting at a wind speed of 10 m/s near the blade root, and for wind speeds greater than 10 m/s, the blade experiences a deep stall from root to tip. Kurhade *et al.*<sup>40-41</sup> numerically investigated how the thermal conductivity of the substrate board affects the temperature control of electronic components. Anant *et al.*<sup>42</sup> experimented with a solar collector made from recycled aluminum cans to dry green chillies. They found that the efficiency of the solar collector decreased as the mass flow rate increased. The highest efficiency of 67.89% was achieved at a mass flow rate of 0.005 kg/s, which effectively removed 88% of the moisture content from the green chillies. Anant *et al.*<sup>43</sup> also conducted a comprehensive study on calophyllum inophyllum biodiesel and dimethyl carbonate blends.

While some studies have focused on either experimental or numerical methods to investigate flow separation control, integrating both approaches could provide a comprehensive understanding. Combined studies could validate computational models and offer insights into complex flow phenomena. Although flow control techniques have been studied for traditional airfoil designs, there's limited research on their application to wind turbine blades. Exploring the efficacy of these techniques in improving wind turbine performance could be valuable. While individual flow control techniques have been explored, research focusing on optimizing multiple techniques for enhanced performance is lacking. Future studies could investigate the synergistic effects of combining different strategies. Although laboratory-scale experiments have shown the effectiveness of various flow control techniques, practical implementation and scale-up for real-world applications remain challenging. Addressing issues like durability, cost-effectiveness, and integration into existing systems could be a focus of future research.

By addressing these research gaps, future studies can contribute to advancing the understanding and application of flow control techniques for improving the

aerodynamic performance of airfoils and wind turbine blades.

## 4.0 Conclusion

Addressing these gaps can lead to significant improvements in aerodynamic performance, benefiting both the aerospace and wind energy industries.

1. Dynamic roughness shows potential in reducing separation bubbles.
2. Its effectiveness at higher angles of attack and elevated Reynolds numbers requires further investigation.
3. Understanding how to scale and practically apply dynamic roughness in real-world situations is crucial.
4. Current research on surface modifications, like dimples and riblets, lacks optimized designs for different conditions.
5. Combining experimental and numerical methods can provide a thorough understanding of flow control techniques.
6. Limited research on applying flow control strategies to wind turbine blades presents a significant opportunity to boost wind energy efficiency.
7. Future studies should focus on optimizing multiple techniques and addressing challenges related to practical implementation.
8. Evaluating the cost-effectiveness and durability of these modifications for long-term use is essential for their successful adoption in the industry.

## 5.0 References

1. Timmer LLWA, Christian Bak. 4 - Aerodynamic characteristics of wind turbine blade airfoils. Brøndsted P, Nijssen R, Goutianos S, editor(s). In woodhead publishing series in energy, advances in wind turbine blade design and materials, 2<sup>nd</sup> ed. Woodhead Publishing; 2023. p. 129-67. <https://doi.org/10.1016/B978-0-08-103007-3.00011-2>.
2. Hajj MR. Wind power and potential for its exploitation in the Arab world. Water, Energy and Food Sustainability in the Middle East. Springer, Cham; 2017. [https://doi.org/10.1007/978-3-319-48920-9\\_11](https://doi.org/10.1007/978-3-319-48920-9_11)
3. Meera SN, Jyothi AL. Innovative multi-directional wind turbine. International Journal and Magazine of Engineering, Technology, Management and Research. 2016; 3(9):1358-65.
4. Hu H. An experimental study of the laminar flow separation on a low-Reynolds-number aerofoil. J Fluids Eng. 2008; 130:051101-1. <https://doi.org/10.1115/1.2907416>
5. Kurhade A et al. Computational study of PCM cooling for the electronic circuit of smartphone. Mater Today: Proc. 2021; 47:3171-6. <https://doi.org/10.1016/j.matpr.2021.06.284>
6. Kurhade AS, Murali G. Thermal control of IC chips using phase change material: A CFD investigation. Int J Mod Phys C. 2022; 33(12). <https://doi.org/10.1142/S0129183122501595>
7. Kurhade AS, Rao TV, Mathew VK, Patil NG. Effect of thermal conductivity of substrate board for temperature control of electronic components: A numerical study. Int J Mod Phys C. 2021; 32(10):2150132. <https://doi.org/10.1142/S0129183121501321>
8. Kurhade AS, Murali G, Rao TV. CFD Approach for thermal management to enhance the reliability of IC chips. Int J Eng Trends Technol. 2023; 71(3):65-72. <https://doi.org/10.14445/22315381/IJETT-V71I3P208>
9. Kurhade AS, Biradar R, Yadav RS, Patil P, Kardekar NB, Waware SY, Munde KH, Nimbalkar AG, Murali G. Predictive placement of IC Chips using ANN-GA approach for efficient thermal cooling. J Adv Res Fluid Mech Therm Sc. 2024; 118(2):137-4. <https://doi.org/10.37934/arfmts.118.2.137147>
10. Upadhe SN, Mhamane SC, Kurhade AS, Bapat PV, Dhavale DB, Kore LJ. Water-saving and hygienic faucets for public places in developing countries. Springer, Cham; 2020. [https://doi.org/10.1007/978-3-030-16848-3\\_56](https://doi.org/10.1007/978-3-030-16848-3_56)
11. Patil SP, Kore SS, Chinchankar SS, Waware SY. Characterisation and machinability studies of aluminium-based hybrid metal matrix composites - A critical review. J Adv Res Fluid Mech Therm Sci. 2023; 101(2):137-63. <https://doi.org/10.37934/arfmts.101.2.137163>
12. Waware SY, Kore SS, Patil SP. Heat transfer enhancement in a tubular heat exchanger with jet impingement: A review. J Adv Res Fluid Mech Therm Sci. 2023; 101(2):8-25. <https://doi.org/10.37934/arfmts.101.2.825>
13. Waware SY, Kore SS, Kurhade AS, Patil SP. Innovative heat transfer enhancement in tubular heat exchanger: An experimental investigation with minijet impingement.

- J Adv Res Fluid Mech Therm Sci. 2024; 116(2), 51-58. <https://doi.org/10.37934/arfmts.116.2.5158>
14. Rahul KS, Kadam PR. Structural behaviour of fillet weld joint for bimetallic curved plate using Finite Element Analysis (FEA). 6th International Conference on Advanced Research in Arts, Science, Engineering and Technology, Organized by DK International Research Foundation, Perambalur, Tamil Nadu ICARASET - 2021 Proceedings/ISBN Number: 978-93-90956-53-1.
  15. Rahul KS, Rao TV. Investigation of mechanical behaviour of laser welded butt joint of Transformed Induced Plasticity (TRIP) steel with effect laser incident angle. Int J Eng Res Technol. 2020; 13(11):3398-403. <https://doi.org/10.37624/IJERT/13.11.2020.3398-3403>
  16. Rahul K, Rao TV, Natu H, Girish HN, Ishigaki T, Madhusudan P. An investigation on laser welding parameters on the strength of TRIP steel, Strojnicki Vestnik/Journal of Mechanical Engineering. 2021; 67(1/2):45-52. <https://doi.org/10.5545/sv-jme.2020.6912>
  17. Rahul KS, Rao TV. Effect of quenching media on laser butt welded joint on Transformed -Induced Plasticity (TRIP). Steel International Journal of Emerging Trends in Engineering Research. 2020; 8(10):7686-91. <https://doi.org/10.30534/ijeter/2020/1588102020>
  18. Khot RS, Rao TV, Keskar A, Girish HN, Madhusudan P. Investigation on the effect of power and velocity of laser beam welding on the butt weld joint on TRIP steel. J Laser Appl. 2020; 32(1):012016. <https://doi.org/10.2351/1.5133158>
  19. Rahul KS, Rao TV, Ishigaki HN, Madhusudan P. An investigation on laser welding parameters and the strength of TRIP steel. Strojnicki Vestnik/Journal of Mechanical Engineering. 2021; 67(1-2):45-52. <https://doi.org/10.5545/sv-jme.2020.6912>
  20. Gadekar TD, Kamble DN, Ambhore NH. Experimental study on gear EP lubricant mixed with Al<sub>2</sub>O<sub>3</sub>/SiO<sub>2</sub>/ZrO<sub>2</sub> composite additives to design a predictive system. Tribol Ind. 2023; 45(4):579-90. <https://doi.org/10.24874/ti.1461.03.23.07>
  21. Kamble DN, Gadekar TD, Agrawal DP. Experimental study on gearbox oil blended with composite additives. J Tribol. 2022; 33:1-19.
  22. Gadekar T, Kamble D. Tribological investigation on oil blended with additive using response surface methodology. E3S Web of Conferences. 2020; 170:0102. <https://doi.org/10.1051/e3sconf/202017001025>
  23. Patil P, Kardekar N, Yadav R, Kurhade A, Kamble D. Al<sub>2</sub>O<sub>3</sub> Nanofluids: An experimental study for MQL grinding. J Mines Met Fuels. 2023; 71(12):2751-6. <https://doi.org/10.18311/jmmf/2023/41766>
  24. Mashud M, Bari AA, Bhowmick TP. Experimental investigation on fluid flow separation control. International Conference on Mechanical Engineering; 2009.
  25. Srivastav D. Flow control over aerofoils using different shaped dimples. IPCSIT. Singapore: IACSIT Press; 2012
  26. Ji-Yaoa, Weibin-Yuanb, Jian-Liang-Wanga, Jianbin-Xiec, Haipeng-Zhoub. Numerical simulation of aerodynamic performance for two-dimensional wind turbine aerofoils. Procedia Eng. 2012; 31:80-6. <https://doi.org/10.1016/j.proeng.2012.01.994>
  27. Bhat SS, Govardhan RN. Stall flutter of NACA0012 aerofoil at low Reynolds numbers. J Fluids Struct. 2013; 41:166-74. <https://doi.org/10.1016/j.jfluidstructs.2013.04.001>
  28. Juanmian L, Feng G, Can H. Numerical study of separation on the trailing edge of a symmetrical aerofoil at a low Reynolds number. Chinese J Aeronaut. 2013; 26(4):918-25. <https://doi.org/10.1016/j.cja.2013.06.005>
  29. Meena DP, Narasimhan PS, Vivek M. Aerodynamic performance of rear roughness aerofoils. The Eighth Asia-Pacific Conference on Wind Engineering, December 10-14, 2013, Chennai, India; 2013 [https://doi.org/10.3850/978-981-07-8012-8\\_252](https://doi.org/10.3850/978-981-07-8012-8_252)
  30. Ghosh P, Dewangan AK, Mitra P, Rout AK. Experimental study of aerofoil with wind tunnel setup. Research Gate. Conference Paper; 2014.
  31. Patel KS, Patel SB, Patel UB, Ahuja AP. CFD analysis of an aerofoil. Int J Eng Res. 2014
  32. Sareen A, Deters RW, Henry SP. Drag reduction using riblet film applied to aerofoil. J Sol Energy Eng. 2014; 136:021007-1. <https://doi.org/10.1115/1.4024982>
  33. Faruqui SHA, AlBari MA, MdEmran, Ferdaus A. Numerical analysis of the role of bumpy surface to control the flow separation of an aerofoil. Procedia Eng. 2014; 90:255-60. <https://doi.org/10.1016/j.proeng.2014.11.846>
  34. Şahin I, Acir A. Numerical and experimental investigations of lift and drag performances of NACA 0015 wind turbine aerofoil. International Journal of Materials, Mechanics and Manufacturing. 2015; 3(1). <https://doi.org/10.7763/IJMMM.2015.V3.159>
  35. Patil B, Thakare H. CFD Analysis of wind turbine blades at various AOA and Low Re. Procedia Eng. 2015; 127:1363-9. <https://doi.org/10.1016/j.proeng.2015.11.495>
  36. Yadav A et al. Design, development and fabrication of horizontal axis wind turbine. 2016 IEEE Students' Conference on Electrical, Electronics and

- Computer Science; 2016. <https://doi.org/10.1109/SCECS.2016.7509359>
37. Dash A. CFD analysis of wind turbine airfoil at various angles of attack. IOSR Journal of Mechanical and Civil Engineering. 2016; 13(4). <https://doi.org/10.9790/1684-1304021824>
38. Tahzib T, Hannan MA, Ahmed YA, Kamal IZM. Performance analysis of H-Darrieus wind turbine with NACA0018 and S1046 aerofoils: Impact of blade angle and TSR. CFD Letters. 2022; 14(2):10-23. <https://doi.org/10.37934/cfdl.14.2.1023>
39. Qaissi K, Elsayed O, Faqir M, Essadiqi E. A validation study of the aerodynamic behaviour of a wind turbine: Three-dimensional rotational case. CFD Letters. 2021; 13(9):1-12. <https://doi.org/10.37934/cfdl.13.9.112>
40. Kurhade AS, Siraskar GD, Bhambare PS, Dixit SM, Waware SY. Numerical investigation on the influence of substrate board thermal conductivity on electronic component temperature regulation. J Adv Res Numer Heat Trans. 2024; 23(1):28-37. <https://doi.org/10.37934/arnht.23.1.2837>
41. Kurhade AS, Kardekar NB, Bhambare PS, Waware SY, Yadav RS, Pawar P, Kirpekar S. A comprehensive review of electronic cooling technologies in harsh field environments: Obstacles, progress, and prospects. J Mine Met Fuel. 2024; 76(2):557-79. <https://doi.org/10.18311/jmmf/2024/45212>
42. Kurhade AS, Waware SY, Munde KH, Biradar R, Yadav RS, Patil P, Patil VN, Dalvi SA. Performance of solar collector using recycled aluminum cans for drying. J Mine Met Fuel. 2024; 72(5):455-61. <https://doi.org/10.18311/jmmf/2024/44643>
43. Kurhade AS, Waware SY, Bhambare PS, Biradar R, Yadav RS, Patil VN. A comprehensive study on *Calophyllum inophyllum* biodiesel and dimethyl carbonate blends: performance optimization and emission control in diesel engines. J Mine Met Fuel. 2024; 72(5):499-507. <https://doi.org/10.18311/jmmf/2024/45188>